

Optimal approach to quantum communication using dynamic programming

Liang Jiang¹, Jacob M. Taylor², Navin Khaneja³, and Mikhail D. Lukin¹

¹*Department of Physics, Harvard University, Cambridge, Massachusetts 02138*

²*Department of Physics, Massachusetts Institute of Technology, Cambridge, Massachusetts 02139 and*

³*School of Engineering and Applied Sciences, Harvard University, Cambridge, Massachusetts 02138*

(Dated: October 25, 2021)

Reliable preparation of entanglement between distant systems is an outstanding problem in quantum information science and quantum communication. In practice, this has to be accomplished via noisy channels (such as optical fibers) that generally result in exponential attenuation of quantum signals at large distances. A special class of quantum error correction protocols—quantum repeater protocols—can be used to overcome such losses. In this work, we introduce a method for systematically optimizing existing protocols and developing new, more efficient protocols. Our approach makes use of a dynamic programming-based searching algorithm, the complexity of which scales only polynomially with the communication distance, letting us efficiently determine near-optimal solutions. We find significant improvements in both the speed and the final state fidelity for preparing long distance entangled states.

INTRODUCTION

Sequential decision making in probabilistic systems is a widely studied subject in the field of economics, management science and engineering. Applications range from problems in scheduling and asset management, to control and estimation of dynamical systems [1]. In this paper we make the first use of these techniques for solving a class of decision making problems that arise in quantum information science [2, 3]. Specifically we consider the optimal design of a so-called quantum repeater for quantum communication. Such repeaters have potential application in quantum communication protocols for cryptography [4, 5, 6] and information processing [7], where entangled quantum systems located at distant locations are used as a fundamental resource. In principle this entanglement can be generated by sending a pair of entangled photons through optical fibers. However, in the presence of attenuation, the success probability for preparing a distant entangled pair decreases exponentially with distance [8].

Quantum repeaters can reduce such exponential scaling to polynomial scaling with distance, and thus provide an avenue to long distance quantum communication even with fiber attenuation. The underlying idea of quantum

repeater [9, 10] is to *generate* a backbone of entangled pairs over much shorter distances, store them in a set of distributed nodes, and perform a sequence of quantum operations which only succeed with finite probability. *Purification* operations [11, 12] improve the fidelity of the entanglement in the backbone, while *connection* operations join two shorter distance entangled pairs of the backbone to form a single, longer distance entangled pair. By relying on a quantum memory at each node to let different sections of the repeater re-attempt failed operations independently, a high fidelity entangled state between two remote quantum systems can be produced in polynomial time. A quantum repeater *protocol* is a set of rules that determine the choice and ordering of operations based upon previous results. An optimal protocol is one that produces entangled pairs of a desired fidelity in minimum time within the physical constraints of a chosen implementation.

The complexity of finding the optimal repeater protocols can be understood via the following analogous example problem [1]: given a sequence of rectangular matrices $M_1 M_2 \dots M_n$, such that M_k is $d_k \times d_{k+1}$ dimensional, find the optimal order of multiplying the matrices such that the number of scalar multiplications is minimized. This is a typical example of a nesting problem, in which the order in which operations are carried out effects the efficiency. For example, if $M_1 = 1 \times 10$, $M_2 = 10 \times 1$ and $M_3 = 1 \times 10$, then $(M_1 M_2) M_3$ takes only 20 scalar operations, while $M_1 (M_2 M_3)$, requires 200 scalar multiplications. A brute force enumeration of all possible nesting strategies and evaluation of their performance is exponential in n . To solve this problem more efficiently, we observe that the optimal nesting strategy $(M_1 \dots (\dots) \dots M_p) (M_{p+1} \dots M_n)$ should carry out the solution to its subparts optimally, i.e., the nesting $(M_1 \dots (\dots) \dots M_p)$ should represent the best nesting strategy for multiplying $M_1 M_2 \dots M_p$. This is the well-known dynamic programming strategy [1], in which one seeks to optimize a problem by comparing different, already optimized sub-parts of the problem. Dynamic programming enables us to find the optimal solution to the original problem in time that is polynomial in n .

Quantum repeaters also have a nested (self-similar) structure, in which shorter distance entanglement is used to create longer distance entanglement, which is then used in turn for further extending the distance between entangled pairs. This structure allows us to use the

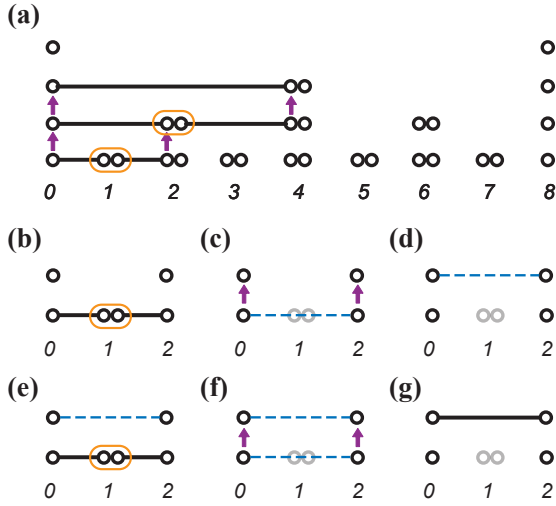


FIG. 1: Quantum repeater scheme from Refs. [9, 10] (BDCZ scheme). (a) In a typical realization with $N + 1 = 9$ nodes, the number of qubits per nodes is bounded by $2 \log_2 2N = 8$. (b)-(d) Two entangled pairs with distance 1 are connected (orange rounded rectangle) at node #1 to produce an entangled state with distance 2, which is stored (purple arrows) in the qubits at higher level. (e)-(g) Another entangled state with distance 2 is produced to purify (purple arrows) the entangled state stored in qubits at higher level. Similarly, entangled states with distance 2^n can be connected to produce entangled state with distance 2^{n+1} , which may be further purified, as indicated in (a).

methods of dynamic programming to find optimal nesting strategies for designing quantum repeater protocols.

We now proceed to detail the specific optimization problem, then discuss our dynamic programming solution to the problem. We next examine two representative schemes that we wish to optimize [the Briegel *et al.* scheme (BDCZ scheme), Refs. [9, 10], and the Childress *et al.* scheme (CTSL scheme), Refs. [13, 14]], and find significant improvements in both preparation time and final fidelity of long distance entangled pairs.

DYNAMIC PROGRAMMING APPROACH

General Quantum Repeater Protocol. Quantum repeater protocols have a *self-similar structure*, where the underlying operations at each stage of the repeater have the same basic algorithms. In other words, the structure of the problem remains the same at each stage, while the parameters can be different. A generic quantum repeater consists of three kinds of operations: entanglement generation, entanglement connection, and entanglement purification. Entangled pairs are first generated and stored over a short distance L_0 . At the first nesting level, two entangled pairs of distance L_0 can be extended

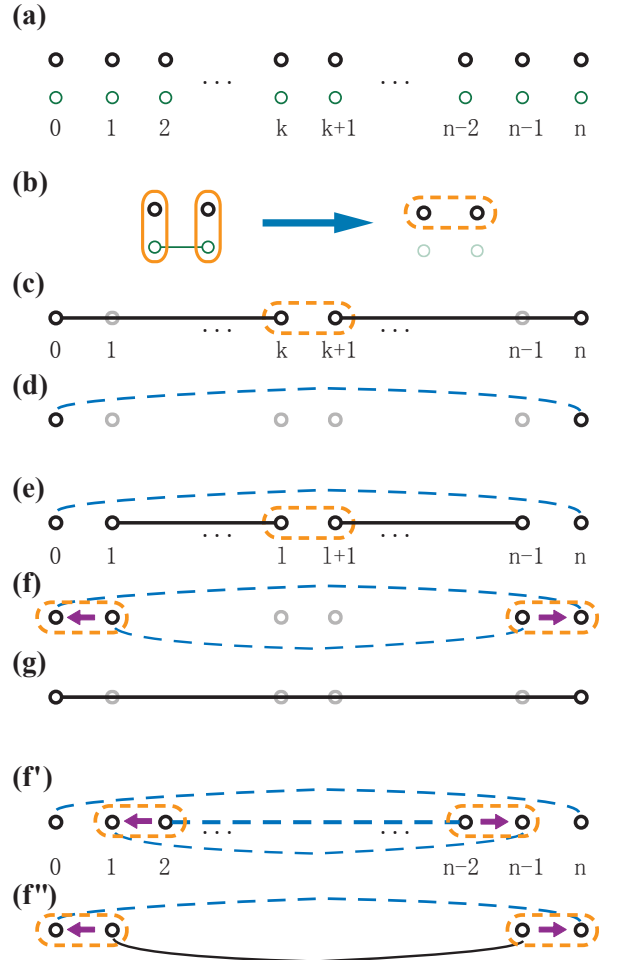


FIG. 2: Quantum repeater scheme from Refs. [13, 14] (CTSL scheme). (a) This scheme has exactly two qubits per node. The communication qubits (green nodes) are used for entanglement generation and short-term storage; the storage qubits (black nodes) are used for long-term storage. (b) With the help of local gates (orange solid rounded rectangles) between communication and storage qubits, the entangled state between communication qubits can be used to implement entangling gates (e.g. the Controlled NOT gate) between storage qubits from neighboring nodes. The effective remote gate is highlighted by the orange dashed rounded rectangle. Such remote gate is sufficient for entanglement connection and purification of storage qubits. The communication qubits are omitted in the following plots. (c)-(d) Entanglement connection to produce an unpurified entangled state with distance n . (e)-(g) Entanglement connection to produce an unpurified entangled state with distance $n - 2$ to purify the entangled state with distance n . (f')(f'') Illustration of multi-level pumping. An entangled state with distance $n - 4$ is used to purify an entangled state with distance $n - 2$, and the (purified) latter is used to purify an entangled state with distance n . The only difference between (f) and (f') is the fidelity of the entangled state with distance $n - 2$. The latter has higher fidelity.

to distance $L_1 \sim 2L_0$ via entanglement connection [6]. Due to limited fidelity of the short pairs and the imperfections from the connection operations, the fidelity of the longer pair produced by connection is generally lower than those of the shorter ones. Nevertheless, the fidelity of the longer pair can be improved via entanglement purification, which is able to extract high-fidelity entangled pairs from an ensemble of low-fidelity ones using operations that are local (restricted to qubits within a given node) [11, 12]. An efficient approach of entanglement purification is entanglement pumping [9, 10], which purifies one and the same pair by using low-fidelity pairs with constant fidelity. [29] Thus, at the $(k+1)$ th nesting level, the three underlying operations (preparation at distance L_k , connection, and purification) lead to preparation at a distance $L_{k+1} \sim 2L_k$. [30]

Inductive Optimization. We now define the optimization problem:

Def: For given physical resources, desired distance L_{final} , and final fidelity F_{final} , an *optimal protocol* minimizes the expected time to have an entangled pair of fidelity $F \geq F_{\text{final}}$ at a distance $L \geq L_{\text{final}}$.

To solve this optimization problem, the choice of parameters for the quantum operation cannot be viewed in isolation—one has to trade off the desire of low present cost (in terms of time) with the undesirability of high future costs. If one tries to enumerate and test all possible adjustable parameters, the complexity to search for the optimized implementation scales at least exponentially with the number of repeater nodes. A simple example is provided if we make our only adjustable parameter choosing between zero and one purification step at each stage of the protocol. For the BDCZ scheme with 128+1 repeater nodes, there are already $2^{128} \gtrsim 10^{38}$ possibilities, which is beyond the capability of current computers. Thus a systematic searching method is needed to find the optimized implementation out of such a huge parameter space.

Based on the above self-similar structure, we may express the optimized protocol to produce long entangled pairs in terms of a set of optimized protocols for producing shorter pairs. The general searching procedure can be performed inductively, as detailed in Table I. We make a discrete set of target fidelities (see Supporting Methods for details), $F = \{f_1, f_2, \dots, f_q\}$, such that only a finite number of different optimal protocols with shorter distances need to be developed. The complexity for each step of our optimization procedure is shown in the table; the full procedure scales as $\mathcal{O}(q^2 n^2)$, where the $\mathcal{O}(n)$ repetitions of step 3 take the most time. [31] In practice, we found the full search of step 3 to be unnecessary—the search can be restricted to pairs of distance $n/2 \pm \mathcal{O}(\log(n))$, leading to complexity $\mathcal{O}(q^2 n \log(n))$.

1. Find and store implementations that optimize the average time (for all fidelities f_1, \dots, f_q) with $dist = n = 1$, taking $\mathcal{O}(q)$
2. Assume known optimized implementations (for all fidelities) with $dist \leq n$
3. Find optimized implementations to produce unpurified pairs (for all fidelities) with $dist = n + 1$ by trying (connecting) all combinations of known optimized implementations with $dist \leq n$, with complexity of order $\mathcal{O}(q^2 n)$
4. Find optimized implementations to produce purified pairs (for all fidelities) with $dist = n + 1$ by trying all combinations of unpurified pairs with $dist = n + 1$, pumping for $m = 0, 1, 2, 3, \dots$ times; complexity goes as $\mathcal{O}(m_{\text{max}} q^2)$
5. Store the optimized implementations (for all fidelities) with $dist = n + 1$, based on step 4.
6. Replace n by $n + 1$, and go to step 2.

TABLE I: Inductive search using dynamic programming

Repeater Schemes and Physical Parameters.

So far, we have only taken a general perspective in explaining quantum repeater protocols and describing the procedure of inductive searching using dynamic programming. In this subsection, we specify the parameters to be optimized by examining the schemes of the quantum repeater, physical restrictions on entanglement generation for current techniques, and the error models of local quantum gates. Only with a functional relationship between physically adjustable parameters and repeater operation outputs, can we find the optimized implementations for procedure 1, 3 and 4 in Table I.

There are several different *schemes* for building a quantum repeater that differ primarily in the amount of physical resources utilized. For example, in the BDCZ scheme [9, 10] (Fig. 1), the maximum number of qubits in the quantum memory (to store intermediate states for connection and purification) required for each repeater node increases logarithmically with the total number of repeater nodes. In the CTSL scheme [13, 14] (Fig. 2), an efficient way to use quantum memory is proposed, and only *two* qubits are needed for each node, regardless of the total number of repeater nodes. One of the two qubits is called the *communication qubit*, which is optically active and can be used to generate entanglement with other communication qubits from neighboring nodes. The other qubit is called the *storage qubit*, which can be used to store quantum state over very long time. As shown in Fig. 2(b), with the help of local gates (orange solid rounded rectangles) between communication and storage qubits, the entangled state between communication qubits can be used to implement teleportation-based gates (e.g., the Controlled NOT gate) between storage qubits from neighboring nodes [7, 24]. Such remote gates (orange dashed rounded rectangle) are sufficient for entanglement connection and purification of the storage qubits; communication qubits are providing the

necessary resource mediating the gates between remote storage qubits. For clarity, we will omit the communication qubits in the following discussion, but still keep track of the mediated operation between remote storage qubits.

To model errors in the physical operations, we need to introduce a number of parameters determined by the quantum hardware. For entanglement generation, the relationship between the fidelity of the elementary pair, F_0 , and the generation time, τ_e , depends on the physical parameters (such as the signal propagation speed, c , the fiber attenuation length, L_{att} , the efficiency of single photon collection and detection, ε , and the distance of elementary pair, L_0) and the specific approach to generate entanglement. For example, for the entanglement generation approach using scattering as proposed in Refs. [13, 14], $F_0 = F_0(\tau_e) = \frac{1}{2} \left\{ 1 + \left[1 - \frac{L_0}{\tau_e c} e^{L_0/L_{att}} \right]^{2(1-\varepsilon)/\varepsilon} \right\}$.

For entanglement connection and pumping, the dominant imperfections are errors from measurement and local two-qubit gate, which we model with a depolarizing channel. In particular, the model for measurement is quantified by a reliability parameter [9, 10], η , which is the probability of faithful measurement. For example, a projective measurement of state $|0\rangle$ would be

$$P_0 = \eta |0\rangle\langle 0| + (1 - \eta) |1\rangle\langle 1|.$$

Similarly, the model for local two-qubit gate is characterized by a reliability parameter [9, 10], p . With probability p , the correct operation is performed; otherwise the state of these two qubits is replaced by the identity matrix [9, 10]. For example, the action on a two qubit operation U_{ij} would be

$$U_{ij} \rho U_{ij}^\dagger \rightarrow p U_{ij} \rho U_{ij}^\dagger + \frac{1-p}{4} \text{Tr}_{ij}[\rho] \otimes I_{ij},$$

where $\text{Tr}_{ij}[\rho]$ is the partial trace over the subsystem i and j , and I_{ij} is the identity operator for subsystem i and j . Generally, the reliability parameters (η and p) should be reasonably high (i.e., above some thresholds [9, 10]), so that the suppression of error from entanglement pumping dominates the new errors introduced by entanglement connection and entanglement pumping. [32]

Optimization Parameters. We now list the adjustable parameters we can optimize over during procedures 1, 3 and 4 in Table I.

1. During the entanglement generation, there is freedom to choose the generation time τ_e , which is determined by the success probability and the communication time. Generally, the higher the success probability, the shorter the generation time and the lower the fidelity of the entangled state, so the generation time and the fidelity should be balanced [13, 14].

2. During the entanglement connection, the distances of two shorter pairs can be adjusted, while the total distance is kept unchanged.

3. During entanglement purification, the number of steps is also adjustable, which should balance the gain in fidelity and the overhead in time.

Additional Operations. Besides the above operations from the original quantum repeater schemes, there are some *additional* operations that might be useful. For example, we may skip several intermediate repeater nodes (*node-skipping*) to generate entanglement between distant nodes directly with a substantially lower success probability. Also, during entanglement pumping, we might consider *multi-level pumping* [15], which is to nest several levels of entanglement pumping together before the next level of entanglement connection (Fig. 2(f')). Multi-level pumping can produce entangled pair with higher fidelity than single-level pumping. Such additional operations can be easily incorporated into the search procedures 1, 3, and 4 in Table I. We will show that the dynamic programming approach can use these additional operations appropriately, to reduce the average time, extend the upper bounds for achievable final fidelity, and even improve the threshold for the reliability parameters of p and η .

RESULTS AND DISCUSSION

Improvement of BDCZ and CTSL Schemes.

With procedure as listed in Table I, we implemented a computer program to examine the mean time to prepare entangled pairs and to search according to our dynamic programming prescription through the parameter space outlined above. We looked for optimal protocols for a quantum repeater for all distances ≤ 1280 km and target fidelities ≥ 0.8 . Unless otherwise specified, we use $L_{att} = 20$ km, $\varepsilon = 0.2$, and $\eta = p = 0.995$ for the rest of the discussion. We first fix $L_0 = 10$ km, and we will consider the optimization of L_0 to justify such choice later. To visualize the results, the profile of the optimized time (smooth surface) is plotted in Fig. 3(a)(b) with respect to the final distance (from 10 km to 1280 km) and the fidelity (from 0.90 to 0.99) for both the BDCZ and the CTSL schemes. The calculation optimizes over the elementary pair generation (both distance and generation time), the connecting positions, and the number of pumping steps, with spacing between neighboring repeater nodes of 10 km; both additional operations (node-skipping and multi-level pumping) are also included for the optimization. For comparison, the unoptimized time profiles (meshes) for the BDCZ and the CTSL schemes are also plotted. The unoptimized protocol assumes fixed elementary pair fidelity ($F_0 = 0.96$ and 0.99 for BDCZ

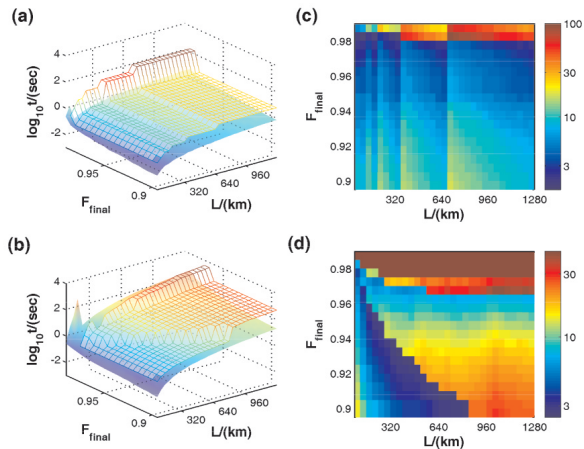


FIG. 3: **Plots of time profiles and improvement factors.** Speed-up in time associated with various final distance and fidelity. (a) $t(F_{\text{final}}, L)$ for unoptimized (meshes) and optimized (smooth surface) implementations of the BDCZ scheme; (b) for the CTSL scheme. (c) Pseudocolor plot of the improvement factor, $t_{\text{unopt}}/t_{\text{opt}}$, for the BDCZ scheme; (d) for the CTSL scheme, in the region ($F_{\text{final}} > 97.5$), the improvement factor $t_{\text{unopt}}/t_{\text{opt}} \rightarrow \infty$. The default parameters are $L_{\text{att}} = 20\text{km}$, $\varepsilon = 0.2$, and $p = \eta = 0.995$.

and CTSL, respectively), simple connection patterns (detailed in Ref. [9, 10] and [13, 14]), and constant number of pumping steps.

As expected, the unoptimized protocol always takes longer time than the optimized protocol for the same final distance and target fidelity. Time profiles for the unoptimized protocols have *stair-like jumps* in Fig. 3(a)(b). For the BDCZ scheme (Fig. 3(a)). The jumps occurring with increasing distance (occurring at distances $L/L_0 = 2^p + 1 = 1, 3, 5, 9, 17, 33, \dots$) are the results of time overhead from the additional level of connection; the jump occurring with at $F_{\text{final}} = 0.98$ is due to the sudden change in the number of pumping steps from 1 to 2. Similarly, for the CTSL scheme (Fig. 3(b)), the two jumps are due to the change of the number of pumping steps from 1 to 2 and finally to 3. For the optimized protocols, the time increases smoothly with increasing final distance and fidelity.

The improvement factor (i.e., the ratio between the times for unoptimized and optimized protocols) is plotted for both the BDCZ and the CTSL schemes in Fig. 3(c)(d). As we might expect, the previously mentioned jumps lead to sharp *stripes* where the improvement factor changes discontinuously. There are several regions where the optimization gives significant improvement. For example, for the BDCZ scheme, the vertical bright stripes indicate that the optimization provides a time-efficient way to generate entangled pairs for distance $(2^p + \delta_+)L_0$ (with $\delta_+ > 0$), gaining a factor of about 10;

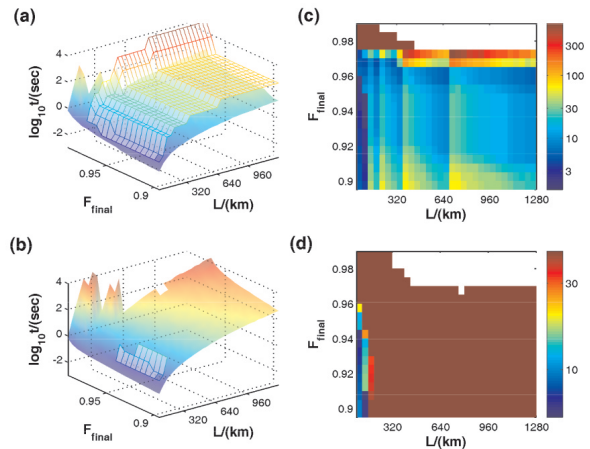


FIG. 4: **Plots of time profiles and improvement factors.** The subplots are arranged in the same way as Fig. 3. Local operations have lower reliability parameters, $p = \eta = 0.990$. (a)(c) For the BDCZ scheme, the optimization procedure only improves the speed of the quantum repeater, and does not extend the achievable region in the F-L plot. (b)(d) For the CTSL scheme, for distances longer than 200km , the improvement factor, $t_{\text{unopt}}/t_{\text{opt}} \rightarrow \infty$. Here, the reliability parameter ($p = \eta = 0.990$) is *insufficient* to create distant entangled pairs with the unoptimized implementation, but the optimized implementation (with multi-level pumping) is still able to create high-fidelity distant entangled pairs, because multi-level pumping lowers the threshold of the reliability parameters for the CTSL scheme.

the horizontal bright stripes indicate that efficiently arranging the number of pumping steps can also speed up the scheme by a factor of about 30 or even more. For most of the optimized protocols, a distant pair is divided into two shorter pairs with similar distance and fidelity (symmetric partition), but occasional asymmetric partitioning can further reduce the time by about 10%.

For the BDCZ scheme, the correspondence between jumps and stripes essentially accounts for all the features of the improvement plot (Fig. 3(c)). For CTSL scheme, however, besides the stripes, there is also a region (with distance $L > 100\text{km}$ and fidelity $F \gtrsim 97.5\%$) where the improvement factor is infinity—optimization not only boosts the speed, but also extends the upper bound of achievable fidelity for distant pairs.

We also study the improvement for other choices of reliability parameters, p and η , especially those values close to the threshold [9, 10]. Suppose the reliability parameters are $p = \eta = 0.990$. In Fig. 4(a)(c), we plot the speed-up in time associated with various final distance and fidelity for the BDCZ scheme. For both (optimized and unoptimized) protocols, the highest achievable fidelity is approximately 97.5% (compared to 99% in Fig. 3(c)), limited by errors from local operations. The improvement factor ranges between [1.5, 600] (compared

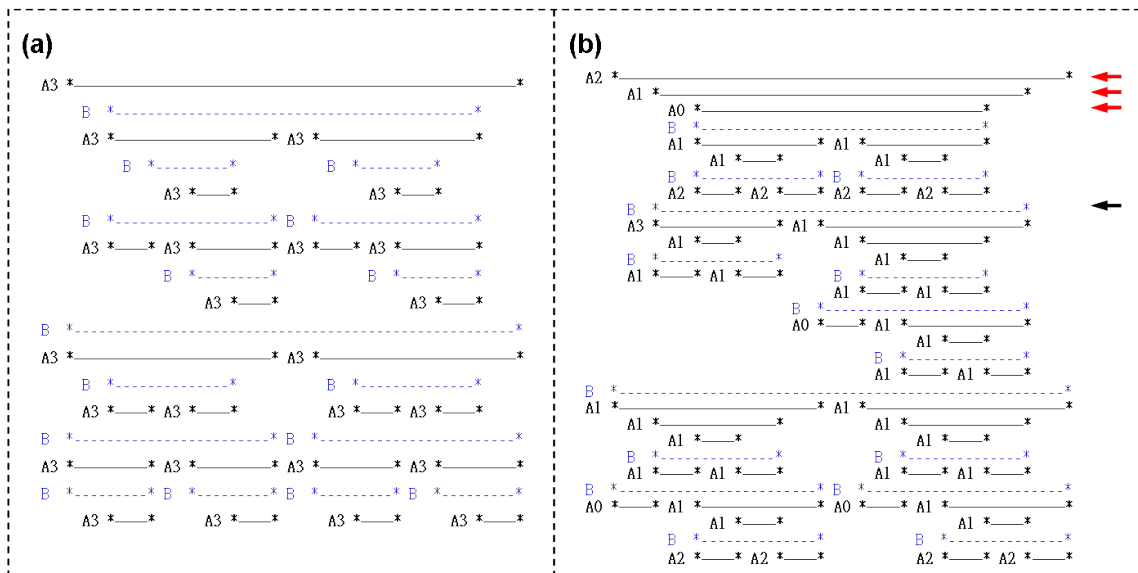


FIG. 5: **Examples.** Two implementations with targeting final distance $L = 11L_0$ and fidelity $F_{final} = 0.976$, using the CTSL scheme. Each storage qubit is represented by “*”. All the relevant entangled states are shown. The order to produce these entangled states are from bottom to top; states on the same row can be produced simultaneously. There are two kinds of entangled states – purified entangled states (type-A, solid black line) and unpurified entangled states (type-B, dashed blue line). On the left side of each purified entangled state, there is a label “Ak”, and this number k indicates that this purified entangled state is obtained from k steps of entanglement pumping. (a) The unoptimized (left) implementation has three pumping steps after each entanglement connection, with average time of about 11 sec to produce the pair wanted. (b) The optimized (right) implementation is from optimization over pair generation time, connection position, and the number of pumping steps. The optimized choice of connection position does not necessarily break the long pair into two almost identical shorter pairs; for example, the entangled state pointed by the black arrow in the 9th row is obtained by connecting two very different shorter pairs in the row below. In addition, the possibility of multi-level pumping is also taken into account during the dynamic programming. As pointed by the red arrows, the pair of storage qubits in the third row pumps the pair in the second row, and the latter pumps the pair in the first row. The average time is about 1.5 sec for the optimized implementation, about 8 times faster than the unoptimized one.

to $[1, 100]$ in Fig. 3(c)). Apart from these differences, the key features (horizontal and vertical stripes) of improvement from optimization are very similar between Fig. 3(c) and Fig. 4(c).

For the CTSL scheme, however, unoptimized and optimized protocols behave very differently, when $p = \eta = 0.990$. As shown in Fig. 4(b)(d), the unoptimized protocol cannot effectively create entangled pairs for distances longer than $200km$, while the optimized protocol is still able to efficiently create distant entangled pairs with very high fidelity. Thus our optimization lowers the threshold requirement for the CTSL scheme of quantum repeater.

To understand the reason for the improvement of the highest achievable fidelity (Fig. 3(d)) and the parameter threshold (Fig. 4(d)), we examine the optimized protocol of CTSL scheme in the next two subsections.

Comparison between Optimized and Unoptimized Protocols. We first compare the detailed procedures between two (optimized and unoptimized) protocols using CTSL scheme to produce a pair with final distance $L = 11L_0$ and fidelity $F_{final} = 97.6\%$, with default reliability parameters $p = \eta = 0.995$. We choose

the highest fidelity achievable by the unoptimized protocol, so that we will see almost all features that give improvements. The results for the unoptimized protocol (Fig. 5(a)) follows Refs. [13, 14] exactly, while the optimized one (Fig. 5(b)) is from our systematic search using dynamic programming. They differ in the following aspects: (1) during entanglement generation, the optimized implementation generates elementary pairs with fidelity lower than 0.99 to reduce the generation time, and uses entanglement pumping afterwards to compensate the fidelity loss; (2) during entanglement connection, the rule of producing long pair from two almost identical shorter pairs is slightly modified (e.g., the pair pointed by the black arrow in the 9th row is from connection of two quite different pairs in the 10th row); (3) the number of pumping steps after each connection varies from 0 to 3 for optimized implementation; (4) finally, the optimized implementation uses multi-level pumping, which will be discussed in detail in the next subsection. For clarity, the additional operation of node-skipping is suppressed in the optimization here. The overall average time is reduced from 11 sec to 1.5 sec, improved by a factor of 8.

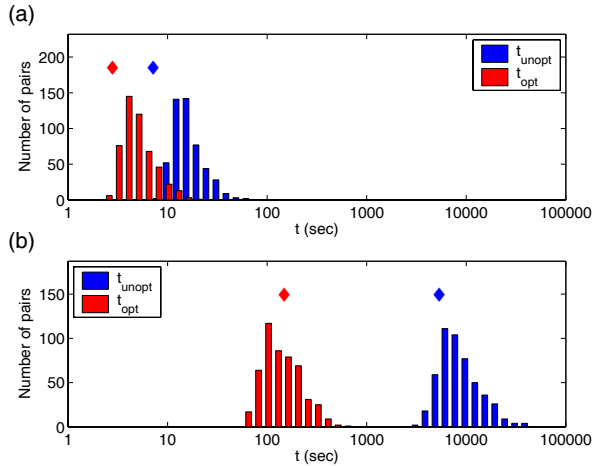


FIG. 6: **Results of Monte Carlo simulation.** Monte Carlo simulation for unoptimized/optimized implementations for (a) the BDCZ scheme and (b) the CTSL scheme, with final distance $1280km$ and fidelity 0.97 . The time distributions for distant pairs are plotted, with red (blue) bars for optimized (unoptimized) implementation. In each plot, the red (blue) diamond indicates the estimated time from average-time approximation for optimized (unoptimized) implementation. The average-time approximation provides a good estimate up to some overall factor ($2 \sim 3$) which is not very sensitive to the implementation.

Note that our optimization results based on average time approximation (see Fig. 6 and Supporting Methods) are confirmed by the Monte-Carlo simulation of the optimized protocols, verifying the substantial speed-up.

Multi-Level Pumping. We now consider the additional operation of multi-level pumping in more detail. We discuss multi-level pumping only for the CTSL scheme, but not for the BDCZ scheme. (In the BDCZ scheme, to introduce multi-level pumping requires additional quantum memory qubits.) In the original unoptimized protocol [13, 14], the purified entangled state with distance n (between the 0th and the n th nodes ($n > 5$)) is produced by entanglement pumping, and the entangled states used for pumping (called pumping-pairs) are *unpurified* entangled states with distance $n - 2$ (Fig. 2(f)). The fidelity of these pumping-pairs with distance $n - 2$ are limited by the connection operation, which imposes an upper-bound for the fidelity of the purified pair with distance n . The underlying restriction is that the pumping-pair is unpurified.

We may lift this restriction by allowing the use of a purified pumping pair. This is multi-level pumping. For example, the pumping-pair with distance $n - 2$ may also be produced by entanglement pumping from pumping-pairs with distance $n - 4$ (Fig. 2(f')), and so on. By doing multi-level pumping, the fidelity of the pumping-pair with distance $n - 2$ is increased (Fig. 2(f')), and the

same for the fidelity upper-bound for the entangled state with distance n . While multi-level pumping can increase the fidelity, it also slows down the repeater scheme.

When the reliability of local operations is above the threshold for the unoptimized protocol (e.g. $p = \eta = 0.995$), we find that multi-level pumping is necessary only for the last two or three levels to the high-fidelity pair we want to produce. Such multi-level pumping can be identified in the optimized implementation – for example, as indicated by red arrows in Fig. 5(b), the pair of storage qubits in the third row pumps the pair in the second row, and the latter pumps the pair in the first row. On the other hand, when the reliability of local operations is below such threshold (e.g. $p = \eta = 0.990$), multi-level pumping is needed almost after every entanglement connection.

If we exclude the possibility of multi-level pumping in dynamic programming, the infinite improvement factor for pairs with distance $L > 100km$ and fidelity $F \gtrsim 97.5\%$ in Fig. 3(d) would disappear. Similarly, in Fig. 4(d), without multi-level pumping, there would be no improvement of the parameter threshold, and even the optimized protocol could not efficiently create distant ($L > 200km$) entangled pairs. For the CTSL scheme, multi-level pumping not only enables us to prepare entangled pairs with very high fidelity, but also lowers the required threshold of the reliability parameters (p and η) for local operations. Therefore, the flexibility to include additional operations in our dynamic programming provides a new perspective on the optimization of quantum repeater schemes.

Other Improvements. In addition to the previously discussed features in the plots of improvement factor, there is an overall improvement for all final distances and fidelities. Such overall improvement comes from the optimized choice of the distance (by node-skipping) and the generation time for *each* elementary pair used. Such overall improvement is about 1.5 (or $2 \sim 3$) for the BDCZ (or CTSL) scheme, which indicates that the original choice of uniform distance $L_0 = 10km$ and initial fidelities $F_0 = 96\%$ (or 99%) are quite close to the optimal.

Finally, we consider if it is possible to gain some additional speed-up if we are allowed to choose the location of the nodes of the quantum repeater. In order to answer this question, we discretize the distance into smaller units, e.g. $1km \ll L_{att}$. Since the distance of each elementary pair is determined by the dynamic programming, the optimized location of the nodes can be inferred from the distances of the elementary pairs. We find that the speed-up due to optimization over the location of the nodes is fairly small, no more than 15% in time (for cases with final distances larger than $200km$). Generally we find that as long as the node spacing is less than the attenuation length ($L_0 < L_{att}$), a quantum repeater can be implemented almost optimally.

Experimental Implications. Throughout our analysis we have assumed relatively high fidelity of local measurements and operations ($\eta = p = 0.995$ or 0.99) and memory times exceeding total communication times. Recent experiments with trapped ions [16, 17], neutral atoms [18], and solid state qubits [19] are already approaching these values of fidelity and memory times. At the same time, high initial entanglement fidelity ($F_0 \approx 96\%$ or 99%) is also needed for the optimized protocols. Entanglement fidelity of about 90% can be inferred from recent experiments with two ions in independent traps [20]. While optimization procedure can yield protocols compatible with fairly low initial fidelity and high local error rates, in practice these errors introduce a large overhead in communication time.

Besides the schemes considered here, there exist other quantum repeater schemes, in particular the Duan *et al.* scheme (DLCZ scheme) [21] that requires a smaller set of quantum operation and relatively modest physical resources. The original DLCZ scheme does not use active entanglement purification and hence cannot correct arbitrary errors. In such a case, optimization is straightforward and has been discussed in [21]. Recently, the DLCZ scheme has been extended to include active entanglement purification in order to suppress e.g. phase noises [22, 23]. The extended DLCZ scheme becomes very similar to the BDCZ scheme in terms of the self-similar structure. The technique of dynamic programming can be applied to optimize the extended DLCZ scheme as well.

CONCLUSION AND OUTLOOK

We have demonstrated how dynamic programming can be a powerful tool for systematically studying the optimization of quantum repeater protocols. We find substantial improvements to two specific repeater schemes [9, 10, 13, 14]. Beyond searching for optimal choices in previously known elements of the schemes (entanglement generation, connection, and pumping), our systematic study can also incorporate more sophisticated additional operations, such as node-skipping, multi-level pumping, and the flexible location of repeater stations. In particular, our multi-level pumping procedure extends the maximum achievable fidelity for distant pairs. It should be possible to include additional possibilities to the optimization problem of quantum repeater, such as different choices of entanglement generation and possibly more efficient usage of local qubits [25, 26]. It would also be interesting to study the optimization problem of quantum repeater with finite storage time of the quantum memory [27, 28]. Even the optimized protocols have a rather limited speed (corresponding to generation of one high-fidelity pair over 1280 km in $1 \sim 100$ s (see Fig. 6)). Therefore, improvement of experimental techniques (to obtain higher local operation fidelities and more efficient atom-photon

coupling) as well as development of new theoretical approaches to speed-up quantum repeaters still remain an outstanding goal. Furthermore, the dynamic programming techniques may find application in other outstanding problems in quantum information science, such as the optimization of quantum error correction for fault tolerant quantum computation. In particular, the optimization of the network-based quantum computation scheme with minimal resources [24] might be possible.

The authors wish to thank Lily Childress and Wolfgang Dur for stimulating discussions. This work is supported by NSF, ARO-MURI, ONR-MURI, the Packard Foundations, and the Pappalardo Fellowship. N.K. acknowledges research support from AFOSR FA9550-05-1-0443, NSF 0133673 and Humboldt foundation.

-
- [1] Bertsekas DP (2000) *Dynamic programming and optimal control* (Athena Scientific, Belmont, Mass).
 - [2] Nielsen MA, Chuang I (2000) *Quantum computation and quantum information* (Cambridge University Press, Cambridge, U.K. ; New York).
 - [3] Bouwmeester D, Ekert AK, Zeilinger A (2000) *The physics of quantum information : quantum cryptography, quantum teleportation, quantum computation* (Springer, Berlin ; New York).
 - [4] Bennett CH, Brassard G, Mermin ND (1992) *Phys Rev Lett* 68:557–559.
 - [5] Bennett CH, Brassard G, Crepeau C, Jozsa R, Peres A, Wootters WK (1993) *Phys Rev Lett* 70:1895–1899.
 - [6] Zukowski M, Zeilinger A, Horne MA, Ekert AK (1993) *Phys Rev Lett* 71:4287–4290.
 - [7] Gottesman D, Chuang IL (1999) *Nature (London)* 402:390–393.
 - [8] Gisin N, Ribordy GG, Tittel W, Zbinden H (2002) *Rev Mod Phys* 74:145–195.
 - [9] Briegel HJ, Dur W, Cirac JI, Zoller P (1998) *Phys Rev Lett* 81:5932–5935.
 - [10] Dur W, Briegel HJ, Cirac JI, Zoller P (1999) *Phys Rev A* 59:169–181.
 - [11] Bennett CH, Brassard G, Popescu S, Schumacher B, Smolin JA, Wootters WK (1996) *Phys Rev Lett* 76:722–725.
 - [12] Deutsch D, Ekert A, Jozsa R, Macchiavello C, Popescu S, Sanpera A (1996) *Phys Rev Lett* 77:2818–2821.
 - [13] Childress L, Taylor JM, Sorensen AS, Lukin MD (2005) *Phys Rev A* 72:052330.
 - [14] Childress L, Taylor JM, Sorensen AS, Lukin MD (2006) *Phys Rev Lett* 96:070504.
 - [15] Dur W, Briegel HJ (2003) *Phys Rev Lett* 90:067901.
 - [16] Leibfried D, DeMarco B, Meyer V, Lucas D, Barrett M, Britton J, Itano WM, Jelenkovic B, Langer C, Rosenband T, *et al.* (2003) *Nature (London)* 422:412–415.
 - [17] Hume DB, Rosenband T, Wineland D (2007) e-Print Archive, <http://arxiv.org/abs/0705.1870>.
 - [18] Beugnon J, Jones MPA, Dingjan J, Darquie B, Messin G, Browaeys A, Grangier P (2006) *Nature (London)* 440:779–782.
 - [19] Dutt MVG, Childress L, Jiang L, Togan E, Maze J,

- Jelezko F, Zibrov AS, Hemmer PR, Lukin MD (2007) *Science* 316:1312-1316.
- [20] Maunz P, Moehring DL, Olmschenk S, Young KG, Matsukevich DN, Monroe C (2007) *Nature Phys* 3:538-541.
- [21] Duan L-M, Lukin MD, Cirac JI, Zoller P (2001) *Nature (London)* 414:413-418.
- [22] Jiang L, Taylor JM, Lukin MD (2007) *Phys Rev A* 76:012301.
- [23] Zhao B, Chen Z-B, Chen Y-A, Schmiedmayer J, Pan J-W (2007) *Phys Rev Lett* 98:240502.
- [24] Jiang L, Taylor JM, Sorensen A, Lukin MD (2007) e-Print Archive, <http://arxiv.org/abs/quant-ph/0703029>.
- [25] van Loock P, Ladd TD, Sanaka K, Yamaguchi F, Nemoto K, Munro WJ, Yamamoto Y (2006) *Phys Rev Lett* 96:240501.
- [26] Ladd TD, van Loock P, Nemoto K, Munro WJ, Yamamoto Y (2006) *New J Phys* 8:184.
- [27] Hartmann L, Kraus B, Briegel HJ, Dur W (2007) *Phys Rev A* 75:032310.
- [28] Collins OA, Jenkins SD, Kuzmich A, Kennedy TAB (2007) *Phys Rev Lett* 98:060502.
- [29] In principle, there exist repeater schemes (see [10] and references therein) that work much faster. For those schemes, however, the number of memory qubits per repeater station scales at least linearly with the final distance, which make them impractical.
- [30] Since we must wait for entanglement generation and purification to succeed before proceeding to the next nesting level, the overall time for successful pair generation is generally much longer than that of classical communication over the given distance.
- [31] For the CTSL scheme, there will be another $\mathcal{O}(q)$ overhead, associated with $\mathcal{O}(q)$ possible fidelity choices of the entangled state for the Controlled NOT gate (Fig. 2b).
- [32] We neglect the time associated with local operations, which is usually much shorter than the communication time between neighboring repeater stations. Non-negligible gate operation time can be easily included in our optimization.

SUPPORTING METHODS: SHAPE PARAMETER APPROXIMATION AND AVERAGE TIME APPROXIMATION

We use two important approximations throughout the analysis: the *shape parameter approximation* and *average*

time approximation.

In the shape parameter approximation [10, 13, 14], we use two numbers, the fidelity and the shape parameter (F, v) to classify non-ideal entangled states during our inductive optimization procedure. For a pair of entangled qubits, we assume that the density matrix is diagonalized in the Bell basis $\rho = \text{diag}(F_1, F_2, F_3, F_4)$, with $F_1 \geq F_2 \geq F_3 \geq F_4$ by an appropriate ordering of the Bell basis. The fidelity $F \equiv F_1$ is the probability of finding the pair in the desired Bell state. The shape parameter $v \equiv \frac{1}{2} \frac{F_3 + F_4}{(F_2 + F_3 + F_4)}$ measures, e.g., the relative ratio of bit error to phase error in the generated pair. We may classify various entangled states according to (F, v) , and use this classification to facilitate the bookkeeping of different states. For intermediate distances, we only keep track of the minimum time (and the associated density matrix) for each class of states labeled by (F, v) , rather than for each possible state. This significantly alleviates the computational storage requirements of dynamic programming. Meanwhile, since we only use a subset of states to optimize longer distance pairs, the obtained protocol might be a little slower (no more than 10%) than the optimal one.

In our average time approximation, we only keep track of the average time for entanglement generation, connection and pumping, instead of the full distribution function. This underestimates the time for entanglement connection, because the average time to generate both sub-pairs is longer than the maximum of the average individual times for two sub-pairs. Fortunately, our comparison between the average time approach and the Monte Carlo simulations show that the average times from the average-time approximation and from Monte Carlo simulations only differ by a factor of about 2 for both the BDCZ and the CTSL schemes. In Fig. 6, the time distributions from Monte Carlo simulation are plotted.